Catalysis Communications 149 (2021) 106234

Contents lists available at ScienceDirect

Catalysis Communications

journal homepage: www.elsevier.com/locate/catcom

High performance of Au/ZTC based catalysts for the selective oxidation of bio-derivative furfural to 2-furoic acid[1]

Georgia Papanikolaou [a], Paola Lanzafame [a,*], Siglinda Perathoner [a], Gabriele Centi [a], Daniela Cozza [b], Gianfranco Giorgianni [b,*], Massimo Migliori [b], Girolamo Giordano [b]

[a] Dept. ChiBioFarAm - Chimica Industriale, University of Messina and ERIC Aisbl, Viale F. Stagno D'Alcontres 31, Messina 98165, Italy
[b] Laboratory of Catalysis and Industrial Chemistry, University of Calabria, Via P. Bucci, I-87036 Rende, Italy

ARTICLE INFO

Keywords:
Zeolite template carbon replica
Selective oxidation
Furfural catalytic upgrading
2-furoic synthesis
Biomass waste valorisation

ABSTRACT

Furfural is a platform bio-molecule for which is valuable to develop new green upgrading processes in bio-refinery. We report here for the first time the high performance of Au/ZTC catalyst for the selective oxidation of furfural to 2-furoic acid, as first step to develop electrodes. The ordered nanostructure and high surface area of BEA structure replica ZTC allows to develop 3D-type electrodes. Au/ZTC catalyst shows higher performance than commercial Vulcan, used as reference conductive carbon in fuel cells. The weak acidity on ZTC avoids decarboxylation and esterification reactions, leading to about 90% of furfural conversion fully selectivity to 2-furoic acid.

1. Introduction

Furfural is a bio-derived platform molecules which further valorisation is of large interest in biorefineries. The selective oxidation of the hydroxylic or aldehydic functionalities to the corresponding carboxylic acids is a very promising way to obtain important building blocks for the production of fine chemicals, new generation bio-fuels and polymers [1–3]. 2,5-furandicarboxylic acid (FDCA), obtained by selective oxidation of 5-hydroxymethylfurfural (HMF), is recognized as one of the top ten value-added products derived from biomass and represents a promising alternative to terephthalic acid (TPA) for the production of bio-based polyethylene 2,5-furandicarboxylate (PEF) [1]. Moreover, 5-hydroxymethyl-2-furancarboxylic acid (HMFCA), another useful building block for the synthesis of polyesters, can be obtained by the selective oxidation of the aldehydic group on HMF [4]. Other relevant synthetic routes involve the conversion of furfural (FF) (Scheme 1). In particular, the selective oxidation of FF to 2-furoic acid (FA), is a relevant industrial reaction, because it represents a step for FDCA production via the Henkel reaction [5] and moreover FA finds high-added-value applications in the pharmaceutical, agrochemical, flavour and fragrance industries. Furthermore, by oxidative esterification with alcohols leads to the formation of green furoate esters which market use is significant increasing [6]. Thus, the selective oxidation of bio-based platform molecules is an important tool for the development of green biorefinery options.

The industrial production of FA from FF is currently performed via the Cannizzaro disproportionation reaction in the presence of NaOH, which requires the addition of sulphuric acid to neutralise the solution, obtaining stoichiometric quantities of furfuryl alcohol (FAOH) and FA, and sodium bisulfate [7]. Direct selective catalytic oxidation with O_2 of FF to FA represents thus a green alternative. Of recent interest, in particular, the possibility to realize the process in an electrocatalytic reactor for the possibility to make the reaction under milder conditions, and especially to couple in tandem with a reductive reaction on the other side of the electrocatalytic reactor to obtain process intensification. However, one of the aspects necessary in this directly is the development of novel 3D-type electrodes to obtain higher accessibility and production rate per unit area of electrode. It is necessary for this to develop 3D type conductive carbon materials which can eventually host metal nanoparticles.

Zeolite-templated carbons (ZTCs), synthesised by using a zeolite as template, are attractive materials for several applications [8] and thanks to their ordered microporous structure and the extremely high surface area, can be considered an interesting support to realize a stable catalyst

* Corresponding author.
E-mail addresses: planzafame@unime.it (P. Lanzafame), gianfranco.giorgianni@unical.it (G. Giorgianni).

[1] This paper in honor of Professor James G. Goodwin, Jr., in the occasion of his 75th birthday, to celebrate his outstanding contribution to catalysis sciences and technology.

https://doi.org/10.1016/j.catcom.2020.106234
Received 9 July 2020; Received in revised form 30 October 2020; Accepted 8 November 2020
Available online 10 November 2020

with a high dispersion of noble metal NPs [9]. Furthermore, the presence of oxygenated groups on the ZTCs surface could play an additional role in the activation of molecular oxygen, as also reported for the oxidation of benzyl alcohol [10]. Their conductive characteristics and the presence of an ordered porous structure is ideal to develop these novel 3D type of electrodes. However, a first step to use them in these electrocatalytic applications is to show how they behaves under thermal catalytic conditions. This is the aim of this study.

Several catalysts based on noble metals supported on different metal oxides were studied in the attempt to develop efficient thermal catalytic systems for the selective oxidation of FF [11]. Quantitative yields to FA were obtained by using supported AuPd/$Mg(OH)_2$ in the presence of NaOH [12], although the use of a base still represents a drawback for the environmental sustainability of the process. Moreover, an additional acidification step is required to convert the obtained furoate to FA. Analogous catalytic systems based on Au nanoparticles (NPs) supported on acidic metals oxides (particularly ZrO_2) were efficiently used for the oxidative esterification of FF with methanol to methyl furoate (MF) in the absence of bases [13,14], because the formation of the esters stabilizes the product and inhibits side reactions. However, the formation of FA rather than MF is preferable from the industrial process perspective, being recovery easier and offering FA a higher variety of utilizations.

In the oxidative esterification, Au NPs promotes the dissociation of O_2 to atomic oxygen able to activate methanol leading to the selective formation of MF through the acetal pathway [13,14]. This acetal pathway, however, is less efficient with respect to the direct oxidation path [2]. The use of Au based catalysts supported on carbon materials, without acidic functionalities on the surface, could hinder the acetals pathway, thus leading to a more efficient catalytic system able to favour the direct oxidation path and the formation of esters. The use of Au/carbon catalysts for the selective oxidation has been scarcely investigated in literature. Only de Jongh and coworkers [15] investigated the oxidation of HMF to HMFCA in aqueous solution and in the presence of a base.

In this communication, we report for the first time the use of ZTC replica of BETA zeolite (β-ZTC) as support for Au NPs, showing high activity and selectivity in the selective oxidation of FF to FA, without using added bases, which can be obtained using this catalyst, compared to the use of a reference materials such as Au NPs supported on a commercial carbon (Vulcan) support. The selection of Vulcan as the carbon support is motivated from being a conductive carbon widely used in fuel cell electrodes, and thus a good reference in view of the development of electrodes for the electrocatalytic selective oxidation of furfurals.

2. Experimental

2.1. Catalysts synthesis and characterization

β-ZTC was synthesised using Na-BEA (Si/Al = 25) as template, via chemical vapour deposition technique [16]. 1.5 g of zeolite was load in a tubular quartz-reactor inserted in a lab-scale furnace (Carbolite GHA 12/1050). Ethylene was used as a carbon source feeding a mixture of this hydrocarbon with a nitrogen-carrier for 4 h at 700 °C (ethylene: 0.03 mol/mol, total flow rate: 500 NmL/min). After carbon deposition, the system underwent a venting step by feeding nitrogen at 700 °C for 1 h. After cooling, β-ZTC was purified [17] by removing the zeolite matrix in a room temperature double step acid-washing procedure: contacting hydrofluoric acid (48% vol, Merck) for 12 h, washing the sample with ultrapure water, then contacting with hydrochloric acid (37% vol, Carlo Erba Reagenti) for 6 h and rinsing the sample again with distilled water. The average yield of ZTC was above 0.4 g for any synthesis.

Gold metal NPs were deposited on β- ZTC and commercial Vulcan (CB Vulcan XC-72 from Cabot Corporation USA) using the sol immobilization method, by suspending 250 mg of carbon support into an aqueous solution containing $HAuCl_4.3H_2O$ (0.013 mmol, Sigma-Aldrich) and polyvinyl alcohol (PVA, Sigma-Aldrich) (Au/PVA = 1:1 wt/wt) as well $NaBH_4$, under continuous stirring for 2 h. The Au-based catalysts (indicated hereinafter as Au/ZTC and Au/Vulcan) were washed, filtered, dried at 80 °C for 12 h and calcined at 200 °C for 2 h in air (heating ramp of 2 °C/min). The final Au-metal loading was 1 wt% [18].

The crystalline structure and of β-ZTC and Au deposited on both supports were analysed by powder XRD (D2 Phaser diffractometer, Bruker) equipped with a Cu tube (λ = 1.54056 Å) and the data recorded in the 2θ range of 5–50° (15°–100° in case of metal deposited samples), with an angular step size of 0.02°.

Textural properties were determined by adsorption/desorption

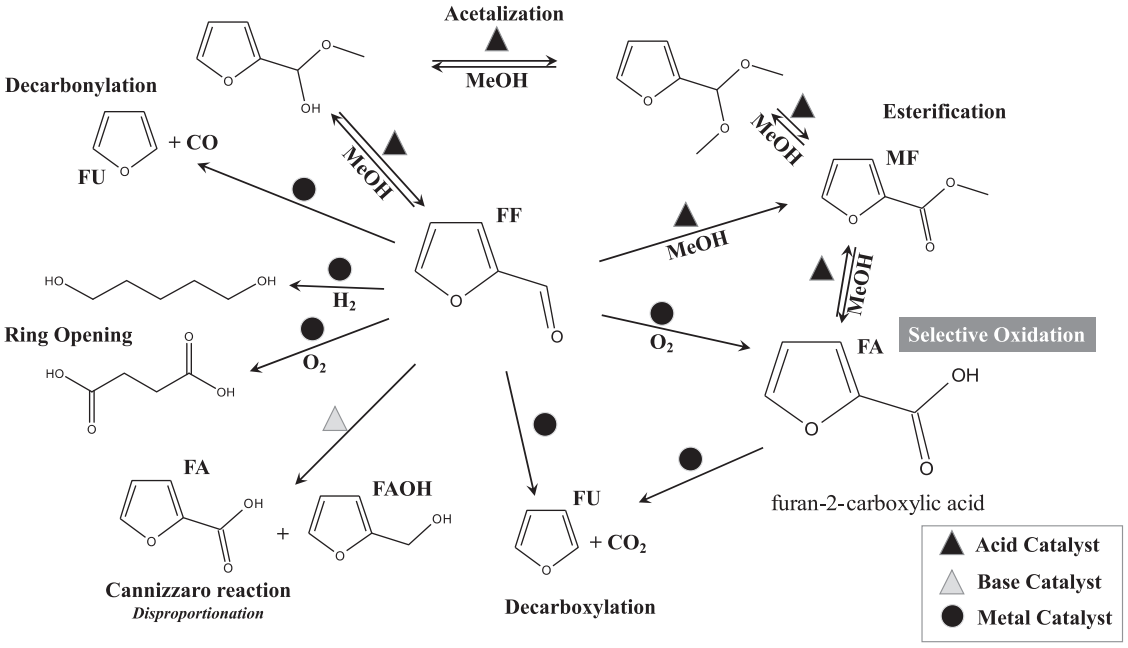

Scheme 1. Furfural conversion pathways

isotherms of N_2 at −196 °C (ASAP2020, Micromeritics). Before each measurement, sample was degassed at room temperature till 50 μmHg, and then, the temperature increased to 350 °C and hold at the end for 6 h. Finally, each sample was cooled to r.t. and backfilled with He. The specific surface area (S_{BET}) was calculated by the Brunauer, Emmett and Teller (BET) method, using the Rouquerol method [19]. The total pore volume was evaluated at p/p° 0.96. The microporous volume and microporous surface area were evaluated by using the t-plot (Harkins and Jura). The pore size distributions (PSD) were calculated by using the HS-2D-NLDFT method, designed for N_2 adsorption on slit-like pores of infinite size present on carbon-based materials (regularization 0.01) [20].

The surface acidity of the samples was determined by NH_3-TPD measurements (TPRO 1000, Thermofisher) by modifying a procedure reported elsewhere [21]. In order to avoid the release of undesired species during NH_3 desorption, 50 mg of sample were loaded in a linear quartz micro-reactor and pre-treated (i.d. 4 mm; length 200 mm) in Helium flow (20 STPmL/min) at 150 °C for 2 h and, then, treated in the range 100–500 °C (ramp 10 °C/min, holding time 30 min) to remove any volatile species from the samples. After that, each sample was treated at 150 °C by a 20 STPmL/min flow of NH_3/He mixture (NH_3: 0.10 mol/mol) for 2 h. Physically adsorbed ammonia was removed by purging in helium at 150 °C until TCD baseline stabilization. Ammonia desorption measurements were then performed in the range 100–700 °C (ramp 10 °C/min, holding time 30 min).

The morphology of the prepared materials was investigated via Scanning Electron Microscopy (SEM) (FEI 200, Quanta) and Transmission Electron Microscopy (TEM) (JEM 1400 Plus, Jeol).

2.2. Catalytic activity assessment

The oxidation of furfural was tested in a 250 mL Teflon-lined stainless-steel autoclave (Parr Instrument Company, 4560 Series) operating in batch mode. 100 mg of catalyst was suspended in a 150 mL methanol solution of furfural (0.02 M). Before each test, the reactor was purged three times by using O_2. Then, at room temperature, the O_2 pressure was increased to 6 barg, the stirring set to 1000 rpm, and, finally, the temperature was increased to 120 °C (15 min). The measured autogenous pressure at 120 °C was 12 barg. The reaction progress was monitored for 6 h by collecting and analysing liquid samples. The collected samples were filtered, and the performance of the reaction measured by GC-FID and GC–MS. Reactant conversion was measured by GC-FID (7890, Agilent) equipped with an auto-sampling device (injected volume 1 μL), DB1 column (Agilent J&W 125–1032, length 30 m, φ = 0.53 mm, film thickness 1.50 μm)). Helium was used as carrier gas (column flow 1.6 mL/min). The oven temperature was increased from 100 to 240 °C (heating rate 25 °C/min), holding the final temperature for 10 min.

Products determination was performed by GC–MS (Agilent 7820A, MSD 5977E), equipped with an auto-sampling device (injected volume 1 μL), HP-5 Column (Agilent, L = 30 m, φ = 0.25 mm, δ = 0.25 μm, Split ratio = 100. Helium was used as carrier gas (column flow 1 mlL/min), and the oven temperature kept at 40 °C for 6 min and then increased to 300 °C (heating rate 10 °C/min) and holding the final isothermal condition for 5 min.

3. Results and discussion

3.1. Characterization

XRD patterns of the synthesised β-ZTC (Supplementary Info) shows a basal peak around 2θ = 7° in the same position as the diffraction of the β-Zeolite. This indicates the presence of regular pores within the structure of carbon like that of the zeolite with a "basal spacing" or periodicity of ≈1.2 nm in the carbon structure [22]. The XRD patterns exhibit a further peak at 2θ = 15°, a position as in β-Zeolite, coherent with a good level of replication of the structure in ordered carbon [22]. The diffraction patterns for Au supported on Vulcan and ZTC catalysts are reported in Fig. 1 revealing the diffraction peaks for metallic cubic gold at 2θ = 38°, 44°, 64° and 78° which corresponds to the crystal planes of (111,200,220) and (311), respectively (JCPDS no.04–0784) [23].

β-ZTC SEM micrographs (Fig. 2) revealed the presence of micron-sized particles, reproducing the crystal morphology of the β-Zeolite scaffold (not shown), while TEM micrographs show the presence of an ordered carbon structures having characteristic dimension of about 0.5 nm (Supplementary Info). SEM micrographs show the presence of a homogeneous dispersion of round-shaped particles of around 100–200 nm, with EDX mapping showing the presence of well dispersed Au in the carbon ZTC matrix (Supplementary Info). No residual Si could be detected, while the presence of O could be revealed, also resulting well dispersed by EDX mapping. TEM images of Au/ZTC and Au/Vulcan (Supplementary Info) show a well dispersion of round-shaped Au nanoparticles with an average size of about 5 nm and comparable in the two samples.

The β-ZTC and Au/ZTC samples present Type Ib/IV N_2 physisorption isotherms (Fig. 3) typical of micro/mesoporous materials, and a hysteresis loop closing above p/p° 0.9, and, apparently, of type H4, typical of particles containing narrow slit-shaped pores [24], due to partial disorder induced in the carbon structure that replicates the full-space of the Na^+-β scaffold [17]. The Au/ZTC sample, with respect to the parent β-ZTC, presents a significant reduction of N_2 adsorption capacity.

The Vulcan XC-72 present a Type Ib/IV isotherm with an H4 and textural features in line with the literature [25]. Among the prepared samples, the β-ZTC presents the largest specific surface area, total pore volume, and micropore volume (Table 1). The latter, in line with the shape of the isotherm, decreased by 28%, 33%, and 30%, respectively, after the deposition of gold, while the external surface area (S_{BET}- S_{mic}) decreased only by 15%. The isotherms do not provide indication about changes in the structure induced by the deposit of Au NPs. The micropore volume is due to a partial pore blocking in the micropore region (Table 1).

The Vulcan support, with respect to the β-ZTC and Au/ZTC samples, shows only a modest microporosity. At the same time, no significant effect on textural properties was observed after Au deposition (Table 1). The pore size distribution for the β-ZTC and Au/ZTC samples (Supplementary Info) show the prevalence of two major families of micropores centered at 9 and 13 Å, respectively, in line with pore openings given by the ideal crystallographic structure of β-ZTC samples [26]. A small amount of irregular mesopores was observed between 50 and 500 Å. Conversely, the Vulcan support presents an irregular pore network with a significant contribution of mesopores centered at 70, 100, and 155 Å, respectively.

NH_3 TPD results (see also Supplementary Info) show that Au/Vulcan has about 70% more acidic sites than Au/ZTC (Table 1), 29.5 with

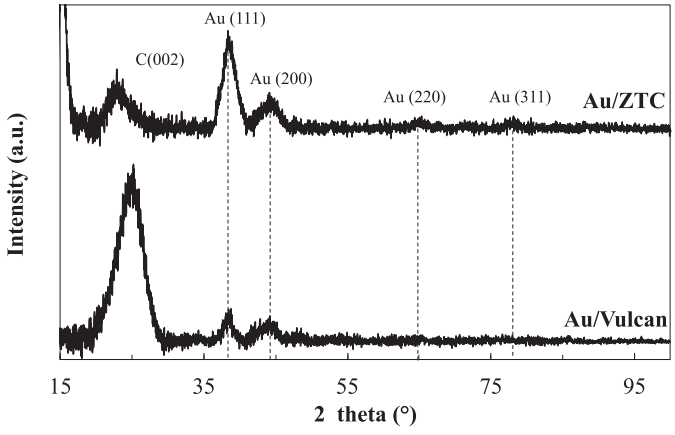

Fig. 1. XRD patterns of the investigated samples after Au deposition.

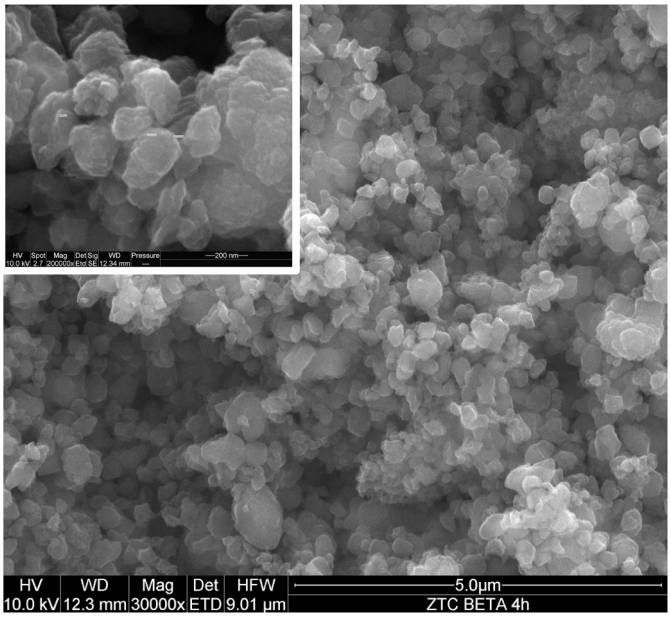

Fig. 2. SEM image of β-ZTC.

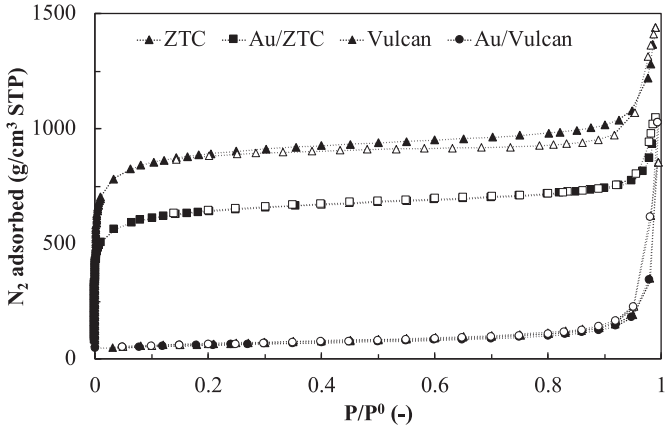

Fig. 3. Porosimetry curve of support and Au-supported samples.

respect to 8.1 µmol/g of acidic sites (Au/Vulcan vs Au/ZTC). The acidity is related to the support and no significant changes are detected after gold loading. NH_3-TPD curves (Supplementary Info) evidence the presence of only weak acidity differently from Vulcan showing stronger acidity. Vulcan acidity is related to the presence of -SO_3H groups in commercial Vulcan, while is surprising the low acidity present in ZTC. Note that SEM data (Supplementary Data) indicate the significant presence of oxygen in the ZTC carbon sample (as well as in the sample before gold loading), differently from the Vulcan sample. Usually the presence of oxygen as heteroatom in carbon samples in an index of acidity, being oxygen typically located at edge sites to form -OH or carboxylic groups. Although some acidity has been detected in ZTC, this is not correspondent to the presence of significant amount of oxygen (about 8–9% wt) which remains as a consequence of the elimination of zeolite template. This indicates that most of this oxygen in not located at accessible edge sites and thus able to give rise to surface acidity.

3.2. Catalytic tests

The catalytic performance of Au/ZTC catalyst was studied in the selective oxidation with O_2 of FF using methanol as solvent and in the absence of added bases. While typically an aqueous medium is used to have a high solubility of the substrate, we instead selected methanol as the solvent to achieve a higher solubility of oxygen in the reaction medium [27]. The catalytic behaviour of Au/ZTC was compared with those of a reference Au/Vulcan catalysts (Fig. 4). As commented in the introduction, we used Vulcan as comparative example, because the aim is to compare the thermal catalytic behaviour of samples which can be used then as catalytic electrodes for the oxidation of bio-based platform molecules. There is thus the need of conductive substrates and Vulcan is the most used carbon substrate for the preparation of electrodes for fuels cells. In addition, Au/Vulcan catalyst behaves better as catalyst for the target reaction with respect other nanocarbon materials, as shown in the Supplementary Info by comparison with the behaviour of Au/CNT, e.g. a sample where Au NPs are deposited on carbon nanotubes.

Data indicates that the ZTC support significantly increases the substrate conversion also at early stages of the reaction, as furfural conversion increases up to 3 h reaching a plateau value of 0.89, due to limitations in oxygen availability. A similar increasing trend over time was observed also by Au/Vulcan even though the maximum conversion was lower than that of Au/ZTC (being present side reactions consuming more oxygen) and the plateau value (0.84) was reached after 5 h of reaction, indicating the slower reaction rate. With respect to selectivity, it is worth to note that GC–MS spectra indicate the presence of only 2-furoic acid as product of reaction at all reaction times. Other products

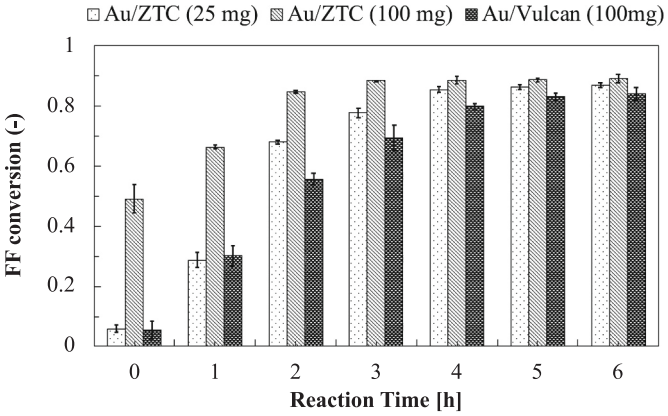

Fig. 4. Furfural conversion evolution over time: effect of carbon support and Au/ZTC catalyst amount.

Table 1
Textural properties of the catalysts.

SAMPLE	Specific Surface Area[a] (m^2/g)	Specific Micropore Surface Area[b] (m^2/g)	Micropore Volume[d] (cm^3/g)	Total Pore Volume[d] (cm^3/g)	Acidity[c] (µmol/g)
Vulcan	235	92	0.04	0.54	29.3
Au/Vulcan	213	86	0.04	0.53	29.5
β-ZTC	3400	2884	1.15	1.90	7.9
Au/ZTC	2433	1998	0.79	1.26	8.1

[a] B.E.T. specific surface area.
[b] Micropore volume calculated by the t-plot method.
[c] From NH_3-TPD profiles.

were not detected. Note that the dimeric acid form cannot be excluded from GC–MS, but the formation of this product seems unlikely.

Among the main possible side products, we can indicate furan, as the product of decarboxylation. The side carboxylic acid is easy to be eliminated in the presence of acid sites [28]. The absence of detection of furan, differently from Au/Vulcan case, confirms the presence of weak acid sites in Au/ZTC. No products deriving from the addition of methanol to the acid (esters), neither of other products deriving from the base-catalysed opening of the aldehydic group in the presence of an alcohol [2], were detected. In addition, humins are a typical by-product observed in furfural oxidation, although often not properly reported. However, this is a main industrial problem, in the conversion of HMF and FF [29]. The absence of humins in Au/ZTC is another advantage of thus catalyst. Furfural derivatives could generate chain α-carbonyl aldehydes through hydrolytic ring opening reaction [30]. This type of products was also not detected, conforming the good properties of Au/ZTC.

The Au/ZTC catalyst show a stable behaviour, at least on a lab-scale experimentations, as shown in the data reported in the Supplementary Info.

Therefore, despite the presence of different side pathways, as further illustrated in Scheme 1, the formation of only FA as product of reaction even using an alcohol as solvent, without thus the typical products observed in the case of oxidative esterification, reveals the unique catalytic properties of Au/ZTC. To note that from an industrial perspective, the use of an alcohol rather than water is highly preferable because significantly lower the energy intensity of the downstream separation unit. Realization of a full selective synthesis of an acid by selective catalytic oxidation in an alcohol solvent is for the first time reported here, as far as we known. The acid could be easy recovered by membrane crystallization [31], which is a low energy separation process, where the use of an alcohol rather than water significantly further improves the energy saving and allow a continuous recirculation of the alcohol solvent. Thus, the innovation introduced using Au/ZTC as a catalyst would reflect also in a significant improvement in terms of green processes for biorefinery.

The absence of furfuryl alcohol supports the point that Cannizzaro reaction (requiring base catalyst) [7] does not takes place in the investigated conditions. As commented before, this is the current industrial process to produce FA, but having various drawbacks both in terms of coproduction and in terms of environmental impact. The absence of furan (FU) in the reaction products remarks the absence of decarboxylation/decarbonylation reactions.

Since esterification or acetalization reactions require acid sites to take place [13,14], the acid obtained as solely product confirms the presence of only weak acidity on Au/ZTC samples, and that FA itself does not act as organocatalyst.

Likely ZTC is not playing only a role as conductive carbon substrate which can host well dispersed Au nanoparticles due to the presence of a well regular nanostructure due to the template synthesis from a zeolite. The presence of large amount of oxygen (deriving from the preparation procedure), but not associated to acid sites such as phenolic or carboxylic sites at edges, indicate the presence of a graphene-oxide surface in the ZTC, with a large presence of C═O or C-O-C non acidic) oxygen sites which are known are responsible in various carbocatalytic reactions [32]. This suggests the interest of metal-free ZTC as novel carbocatalyst.

The presence of large amount of oxygen (about 6–9 wt%) with minimal surface acidity could be attributed to the specific structure of this support. The pore connectivity of the zeolite support, imposes a curvature of the graphene sheet, leading to the formation of carbon edge sites, highly unstable which can react with water during the template removal process [33]. Epoxy, carbonyl and lactone groups are thus predominantly present on the ZTC support in a higher amount with respect to other nanocarbon materials. Although the analysis and demonstration of these aspects is not part of this communication, we could anticipate as preliminary indication that ZTC are an interesting novel class of carbocatalysts for other applications.

Another relevant evidence of Fig. 4 is the initial activity of the Au/ZTC samples showing ca. 0.5 conversion at reaction close to zero. Zero is the time when the autoclave reaches the reaction temperature of 120 °C ± 2 °C (about 15 min). Thus, in Au/ZTC already during this step, conversion of FF begins, whilst for Au/Vulcan the initial conversion results close to zero. Looking for another proof of the initial Au/ZTC activity, a test was also performed by loading 25 mg of catalyst. Note that the catalyst to substrate (FF) ratio in these conditions decreases from about 0.35 to 0.09 wt. With respect to the total volume of reaction, the catalyst amount passes from 1185 to 4740 times lower. Thus, the amount of catalyst is quite low in these experiments, confirming the high activity. Au/ZTC catalyst presents high stability in the investigate conditions and no evidence of reactivity loss was observed (Supplementary Info).

By using 25 mg of catalyst (Fig. 4), the conversion increases slowly with respect to the test with 100 mg of Au/ZTC, with a 0.06 conversion at reaction time = 0 and a conversion plateau (0.86 close to that reached with higher catalyst amount) achieved after 4 h of reaction. These results confirm that Au/ZTC is very active and shows a promising activity in furfural oxidation toward 2-furoic acid. Note that we have used here a reaction temperature of 120 °C to have comparable data with earlier studies on Au/ZrO_2 catalysts [5,6,13,14,34]. The comparison with literature data using oxide supports for Au confirm the higher performances (activity, selectivity) of Au NPs supported on ZTC with respect to other supports.

4. Conclusions

We report here for the first time the very high performances of Au/ZTC catalysts in the selective oxidation of FF in the absence of an added base, and the peculiar ability to form the acid rather than the ester using methanol as a solvent. This has many positive implications in terms of industrial development of this green chemical synthesis of interest for biorefinery areas.

A highly performing catalyst for the selective oxidation of furfural to furoic acid was obtained by depositing Au nanoparticles on β-ZTC carbon prepared by carbon replica of BETA zeolite. The comparison of the catalytic performance of Au/Vulcan and Au/ZTC catalysts shows that the use of ZTC support significantly increases the conversion of furfural also at early stages of the reaction, with an increase of FF conversion up to 3 h reaching a plateau value of 0.89, with total selectivity toward the formation of FA. The presence of only weak acid sites on the supports hinders the acetalization and esterification pathways, favouring the selective oxidation of the aldehydic functionality on the furan ring. Further studies are in progress to assess the exact role of the ZTC support on the overall catalytic performance of the Au/ZTC catalyst and their use also as metal-free carbocatalyst, with the first results giving indications of an active role in the mechanism in addition to the role of stabilization of well dispersed Au NPs and the possibility to develop novel electrocatalysts for bio-based platform molecules conversion. The relatively large amount of oxygen on the external surface could play a key role in the mechanism of conversion, confirming the peculiar properties of these carbon materials with respect to other type of nanocarbon materials [32].

Funding

No funding was received for this work.

Declaration of Competing Interest

The authors declare that they have no known competing financial interests or personal relationships that could have appeared to influence the work reported in this paper.

Acknowledgments

Prof. Lorenzo Caputi (University of Calabria, Italy) and CNR-IMM (Catania, Italy) are kindly acknowledged for HR-TEM image.

The authors also thank the support of PRIN2017 project CO_2 ONLY (project nr. 2017WR2LRS) and part also the support of the EU project PERFORM (project 820723).

Appendix A. Supplementary data

Supplementary data to this article can be found online at https://doi.org/10.1016/j.catcom.2020.106234.

References

[1] R. Mariscal, P. Maireles-Torres, M. Ojeda, I. Sádaba, M. López Granados, Energy Environ. Sci. 9 (2016) 1144–1189. https://doi.org/10.1039/C5EE02666K.

[2] a) P. Lanzafame, G. Papanikolaou, K. Barbera, G. Centi, S. Perathoner, Etherification of HMF to biodiesel additives: The role of NH_4^+ confinement in Beta zeolites, J. Energy Chem. 36 (2019) 114–121, https://doi.org/10.1016/j.jechem.2019.07.009;
b) P. Lanzafame, G. Papanikolaou, S. Perathoner, G. Centi, M. Migliori, E. Catizzone, A. Aloise, G. Giordano, Direct versus acetalization routes in the reaction network of catalytic HMF etherification, Catal. Sci. Technol. 8 (2018) 1304–1313, https://doi.org/10.1039/C7CY02339A.

[3] F.H. Isikgor, C.R. Becer, Lignocellulosic biomass: a sustainable platform for the production of bio-based chemicals and polymers, Polym. Chem. 6 (2015) 4497–4559, https://doi.org/10.1039/C5PY00263J.

[4] A.F. Sousa, C. Vilela, A.C. Fonseca, M. Matos, C.S.R. Freire, G.-J.M. Gruter, J.F. J. Coelho, A.J.D. Silvestre, Biobased polyesters and other polymers from 2,5-furandicarboxylic acid: a tribute to furan excellency, Polym. Chem. 6 (2015) 5961–5983, https://doi.org/10.1039/C5PY00686D.

[5] C.P. Ferraz, A.H. Braga, M.N. Ghazzal, M. Zieliński, M. Pietrowski, I. Itabaiana, F. Dumeignil, L.M. Rossi, R. Wojcieszak, Efficient oxidative esterification of furfural using au nanoparticles supported on group 2 alkaline earth metal oxides, Catalysts 10 (2020) 430, https://doi.org/10.3390/catal10040430.

[6] R. Radhakrishnan, S. Thiripuranthagan, A. Devarajan, S. Kumaravel, E. Erusappan, K. Kannan, Oxidative esterification of furfural by au nanoparticles supported CMK-3 mesoporous catalysts, Appl. Catal. A Gen. 545 (2017) 33–43, https://doi.org/10.1016/j.apcata.2017.07.031.

[7] C.D. Hurd, J.W. Garrett, E.N. Osborne, Furan reactions. IV. Furoic acid from furfural, J. Am. Chem. Soc. 55 (1933) 1082–1084, https://doi.org/10.1021/ja01330a032.

[8] M.R. Benzigar, S.N. Talapaneni, S. Joseph, K. Ramadass, G. Singh, J. Scaranto, U. Ravon, K. Al-Bahilyc, A. Vinu, Recent advances in functionalized micro and mesoporous carbon materials: synthesis and applications, Chem. Soc. Rev. 47 (2018) 2680–2721, https://doi.org/10.1039/C7CS00787F.

[9] Y. Yang, L. Tang, N. Burke, K. Chiang, Nanoporous carbon supported metal particles: their synthesis and characterisation, J. Nanopart. Res. 14 (2012) 1028–1040, https://doi.org/10.1007/s11051-012-1028-9.

[10] J. Zhu, S.A.C. Carabineiro, D. Shan, J.L. Faria, Y. Zhu, J.L. Figueiredo, Oxygen activation sites in gold and iron catalysts supported on carbon nitride and activated carbon, J. Catal. 274 (2010) 207–214, https://doi.org/10.1021/acscatal.7b00829.

[11] a) A.P. Dunlop, Process for manufacturing furoic acid and furoic acid salts, US Patent (1946), 2407066;
b) Q.Y. Tian, D.X. Shi, Y. Sha, CuO and Ag_2O/CuO catalyzed oxidation of aldehydes to the corresponding carboxylic acids by molecular oxygen, Molecules 13 (2008) 948–957, https://doi.org/10.3390/molecules13040948.

[12] M. Douthwaite, X. Huang, S. Iqbal, P.J. Miedziak, G.L. Brett, S.A. Kondrat, J. K. Edwards, M. Sankar, D.W. Knight, D. Bethell, G.J. Hutchings, The controlled catalytic oxidation of furfural to furoic acid using AuPd/$Mg(OH)_2$, Catal. Sci. Technol. 7 (2017) 5284–5293, https://doi.org/10.1039/C7CY01025G.

[13] M. Signoretto, F. Menegazzo, L. Contessotto, F. Pinna, M. Manzoli, F. Boccuzzi, Au/ZrO_2: an efficient and reusable catalyst for the oxidative esterification of renewable furfural, Appl. Catal. B: Environ. 129 (2013) 287–293, https://doi.org/10.1016/j.apcatb.2012.09.035.

[14] F. Pinna, A. Olivo, V. Trevisan, F. Menegazzo, M. Signoretto, M. Manzoli, F. Boccuzzi, The effects of gold nanosize for the exploitation of furfural by selective oxidation, Catal. Today 203 (2013) 196–201, https://doi.org/10.1016/j.cattod.2012.01.033.

[15] B. Donoeva, N. Masoud, P.E. de Jongh, Carbon support surface effects in the gold-catalyzed oxidation of 5-hydroxymethylfurfural, ACS Catal. 7 (2017) 4581–4591, https://doi.org/10.1021/acscatal.7b00829.

[16] T. Kyotani, Z. Ma, A. Tomita, Template synthesis of novel porous carbons using various types of zeolites, Carbon 41 (2003) 1451–1459, https://doi.org/10.1016/S0008-6223(03)00090-3.

[17] L. Tosheva, J. Parmentier, V. Valtchev, C. Vix-Guterl, J. Patarin, Carbon spheres prepared from zeolite Beta beads, Carbon 43 (2005) 2474–2480, https://doi.org/10.1016/j.carbon.2005.04.030.

[18] A. Villa, D. Wang, G.M. Veith, F. Vindigni, L. Prati, Sol immobilization technique: a delicate balance between activity, selectivity and stability of gold catalysts, Catal. Sci. Technol. 3 (2013) 3036–3041, https://doi.org/10.1039/C3CY00260H.

[19] M. Thommes, K. Kaneko, A.V. Neimark, J.P. Olivier, F. Rodriguez-Reinoso, J. Rouquerol, K.S.W. Sing, Physisorption of gases, with special reference to the evaluation of surface area and pore size distribution (IUPAC Technical Report), Pure Appl. Chem. 87 (2015) 1051–1069, https://doi.org/10.1515/pac-2014-1117.

[20] J. Jagiello, J.P. Olivier, 2D-NLDFT adsorption models for carbon slit-shaped pores with surface energetical heterogeneity and geometrical corrugation, Carbon 55 (2013) 70–80, https://doi.org/10.1016/j.carbon.2012.12.011.

[21] E. Catizzone, Z. Cirelli, A. Aloise, P. Lanzafame, M. Migliori, G. Giordano, Methanol conversion over ZSM-12, ZSM-22 and EU-1 zeolites: from DME to hydrocarbons production, Catal. Today 304 (2018) 39–50, https://doi.org/10.1016/j.cattod.2017.08.037.

[22] Z. Yang, Y. Xia, R. Mokaya, Enhanced hydrogen storage capacity of high surface area zeolite-like carbon materials, J. Am. Chem. Soc. 129 (2007) 1673–1679, https://doi.org/10.1021/ja067149g.

[23] Joint Committee of Powder Diffraction Standards, Diffraction Data File, JCPDS International Center for Diffraction Data. Swarthmore PA, 1991.

[24] K.S.W. Sing, D.H. Everett, R.A.W. Haul, L. Moscou, R.A. Pierotti, J. Rouquerol, T. Siemieniewska, Reporting physisorption data for gas/solid systems, in: Handbook Heterog. Catal, Wiley-VCH Verlag GmbH & Co. KGaA, Weinheim, Germany, 2008, https://doi.org/10.1002/9783527610044.hetcat0065.

[25] B. Liu, S. Creager, Carbon xerogels as Pt catalyst supports for polymer electrolyte membrane fuel-cell applications, J. Power Sources 195 (2010) 1812–1820, https://doi.org/10.1016/j.jpowsour.2009.10.033.

[26] E. Braun, Y. Lee, S.M. Moosavi, S. Barthel, R. Mercado, I.A. Baburin, D. M. Proserpio, B. Smit, Generating carbon schwarzites via zeolite-templating, Proc. Natl. Acad. Sci. U. S. A. 115 (2018) E8116–E8124, https://doi.org/10.1073/pnas.1805062115.

[27] R. Battino, T.R. Rettich, T. Tominaga, The solubility of oxygen and ozone in liquids, J. Phys. Chem. Ref. Data 12 (1983) 163–178, https://doi.org/10.1063/1.555680.

[28] X.Y. Toy, I.I.B. Roslan, G.K. Chuah, S. Jaenicke, Protodecarboxylation of carboxylic acids over heterogeneous silver catalysts, Catal. Sci. Technol. 4 (2014) 516–523, https://doi.org/10.1039/C3CY00580A.

[29] G. Tsilomelekis, M.J. Orella, Z. Lin, Z. Cheng, W. Zheng, V. Nikolakis, D.G. Vlachos, Molecular structure, morphology and growth mechanisms and rates of 5-hydroxymethyl furfural (HMF) derived humins, Green Chem. 18 (2016) 1983–1993, https://doi.org/10.1039/C5GC01938A.

[30] N. Shi, Q. Liu, H. Cen, R. Ju, X. He, L. Ma, Formation of humins during degradation of carbohydrates and furfural derivatives in various solvents, Biomass Conversion and Biorefinery 10 (2020) 277–287, https://doi.org/10.1007/s13399-019-00414-4.

[31] R. Salmón, P. Luis, Membrane crystallization via membrane distillation, Chem. Eng. Proc. - Process Intensification 123 (2018) 258–271, https://doi.org/10.1016/j.cep.2017.11.017.

[32] (a) D.S. Su, S. Perathoner, G. Centi, Nanocarbons for the development of advanced catalysts, Chem. Rev. 113 (2013) 5782–5816, https://doi.org/10.1021/cr300367d;
b G. Centi, S. Perathoner, D.S. Su, Nanocarbons: opening new possibilities for nano-engineered novel catalysts and catalytic electrodes, Catal. Surveys from Asia 18 (2014) 149–163, https://doi.org/10.1007/s10563-014-9172-0.

[33] H. Nishihara, Q.H. Yang, P.X. Hou, M. Unno, S. Yamauchi, R. Saito, J.I. Paredes, A. Martìnez-Alonso, J.M.D. Tascòn, Y. Sato, M. Terauchi, T. Kyotani, A possible buckybowl-like structure of zeolite templated carbon, Carbon 47 (2009) 1220–1230, https://doi.org/10.1016/j.carbon.2008.12.040.

[34] C. Ampelli, K. Barbera, G. Centi, C. Genovese, G. Papanikolaou, S. Perathoner, K. J. Schouten, J.K. van der Waal, On the nature of the active sites in the selective oxidative esterification of furfural on Au/ZrO_2 catalysts, Catal. Today 278 (2016) 56–65, https://doi.org/10.1016/j.cattod.2016.04.023.